

# Eliminating experimental bias in anisotropic-flow measurements of high-energy nuclear collisions

Matthew Luzum, Jean-Yves Ollitrault

CNRS, URA2306, IPhT, Institut de physique theorique de Saclay, F-91191 Gif-sur-Yvette, France

(Dated: November 27, 2024)

We argue that the traditional event-plane method, which is still widely used to analyze anisotropic flow in ultrarelativistic heavy-ion collisions, should be abandoned because flow fluctuations introduce an uncontrolled bias in the measurement. Instead, one should use an alternative, such as the scalar-product method or cumulant method, which always measures an unambiguous property of the underlying anisotropic flow and therefore eliminates this bias, and does so without any disadvantages. It is known that this correction is important for precision comparisons of traditional  $v_n$  measurements requiring better than a few percent accuracy. However, we show that it is absolutely essential for correlations between different harmonics, such as those that have been recently measured by the ATLAS Collaboration, which can differ from the nominally-measured quantity by a factor two or more. We also describe how, using the corrected analysis method, the information from different subevents can be combined in order to optimize the precision of analyses.

## I. INTRODUCTION

Anisotropic flow  $v_n$ , in particular elliptic flow  $v_2$ , is one of the most important observables of ultrarelativistic heavy-ion collisions [1–8]. It is therefore important to devise the best possible methods to analyze it. A good measurement should be reproducible; in particular, it should be done in such a way that one can easily compare results from different experiments, using different detectors. For the sake of comparison with theory, an ideal measurement is a well-defined quantity that corresponds to a generic property of the system, closely related to an interesting theoretical concept. Any such measurement is superior to one that lacks these traits.

In this paper, we argue that the traditional event-plane method [9], which is still used by most of the major experimental collaborations [7, 8, 10–12] does not satisfy any of the above requirements defining a good measurement. When the method was first developed, it was assumed that event-by-event fluctuations in  $v_n$  were negligible. However, it is now known that  $v_n$  fluctuates significantly within a class of events [13–15]. As a result, an event-plane measurement of  $v_n$  yields an ambiguous measure lying somewhere between the event-averaged mean value  $\langle v_n \rangle$  and the root-mean-square value  $\langle v_n^2 \rangle^{1/2}$  [16, 17]. Where exactly depends on the “resolution”, which strongly depends on the experimental setup. This means that, e.g., the same Pb-Pb collisions at the LHC yield a systematically different value of  $v_n$  depending on whether they are analyzed by ALICE, CMS or ATLAS, and that comparisons to earlier measurements from lower energy collisions at RHIC are ambiguous. The difference is typically of a few percent for elliptic flow [17], but is larger for higher harmonics like triangular flow  $v_3$  [15], which is solely due to fluctuations.

Fortunately, there exist alternative analysis methods that do not suffer from this ambiguity, such as the two-particle cumulant method [18, 19] or a slight variant of the traditional event-plane method called the

scalar-product method introduced by the STAR collaboration [20]. These make for a superior measurement because they consistently yield the rms value of  $v_n$ , while introducing no disadvantage compared to the traditional event-plane measurements. Supplemented by higher order cumulant measurements, these make traditional event-plane measurements completely redundant, as they contain no independent information about the underlying flow.

Traditional event-plane analysis methods have also been used to measure higher-order, mixed-harmonic correlations [21–23]. These measurements also suffer from similar biases as traditional event-plane  $v_n$  measurements, but in this case they are much larger [24], causing significant problems even for qualitative comparisons. Fortunately, these problems can be repaired with a few simple changes.

In Secs. II A and II B, we recall the principle of the traditional event-plane method and of its variant, the scalar-product method. In Sec. II C, we show that the former yields an ambiguous measurement in the presence of flow fluctuations, while the latter yields an unambiguous result. These results are already known to experts [16]. For purposes of illustration, we make several simplifications compared to what is typically done in an experiment, and in Sec. II D discuss these complications and why they do not change the results. We also describe in Sec. II E a new, systematic way of improving the accuracy of the scalar-product method by combining reference flows from “subevents”. In Sec. III, the discussion is extended to the analysis of mixed correlations, where we show for the first time that the ambiguity resulting from flow fluctuations is much larger, and the proposed corrected procedure is therefore critical.

## II. MEASURING $v_n$

The picture underlying anisotropic flow measurements is that, if the system exhibits strong collective behavior

(i.e., “flow”), particles in each event are emitted independently according to an underlying one-particle probability distribution [25]

$$\frac{2\pi}{N} \frac{dN}{d\phi} = 1 + 2 \sum_{n=1}^{\infty} v_n \cos n(\phi - \Phi_n), \quad (1)$$

where  $\phi$  is the azimuthal direction of an emitted particle,  $v_n$  is the amplitude of anisotropic flow in the  $n$ th harmonic, and  $\Phi_n$  the corresponding reference angle. Further assumptions underlying most analyses are that  $\Phi_n$  represents a global angle that depends little on pseudorapidity and transverse momentum, that event-by-event fluctuations of  $v_n$  also depend little on pseudorapidity and transverse momentum, and that multiplicity fluctuations within a centrality bin are negligible.

Experiments typically detect anywhere from a few hundred particles to at most a few thousand in a given collision event, while the anisotropy coefficients  $v_n$  are typically a few percent or less. A precise reconstruction of the underlying probability distribution is therefore impossible in a single event. Information about the underlying probability distribution can only be extracted from (azimuthally symmetric) correlations between outgoing particles, averaged over a large ensemble of events [26].

### A. The flow vector

The various experimental estimates of  $v_n$  have compact expressions in terms of the flow vector  $\vec{Q}_n$  in harmonic  $n$ . For a given set of  $N$  particles belonging to the same event, one defines  $\vec{Q}_n \equiv (|Q_n| \cos(n\Psi_n), |Q_n| \sin(n\Psi_n))$  by [9]

$$\begin{aligned} |Q_n| \cos(n\Psi_n) &= \frac{1}{N} \sum_j \cos(n\phi_j) \\ |Q_n| \sin(n\Psi_n) &= \frac{1}{N} \sum_j \sin(n\phi_j), \end{aligned} \quad (2)$$

where the sum runs through the set of  $N$  particles with respective azimuthal angles  $\phi_j$ . The flow vector (2) can also be written in complex form

$$Q_n = |Q_n| e^{in\Psi_n} \equiv \frac{1}{N} \sum_j e^{in\phi_j}. \quad (3)$$

The original idea behind the event-plane method is that the direction  $\Psi_n$  of the flow vector in a reference detector provides an estimate of the corresponding angle  $\Phi_n$  in the underlying probability distribution [27]. Because a finite sample of particles is used, statistical fluctuations cause  $\Psi_n$  to differ from  $\Phi_n$ . This dispersion is characterized by the “resolution”, defined as:

$$R \equiv \left\langle e^{in(\Psi_n - \Phi_n)} \right\rangle = \left\langle \frac{Q_n}{|Q_n|} e^{-in\Phi_n} \right\rangle, \quad (4)$$

where angular brackets denote an average over events. Note that this average is real by parity symmetry, except for irrelevant statistical fluctuations.

When the method was developed, it was assumed that dynamical fluctuations of the underlying probability distribution are negligible, so that  $v_n$  is the same for all events. We then rewrite Eq. (4) as

$$R(v_n) \equiv \left\langle e^{in(\Psi_n - \Phi_n)} \right\rangle_{|v_n} = \left\langle \frac{Q_n}{|Q_n|} e^{-in\Phi_n} \right\rangle_{|v_n}. \quad (5)$$

where  $\langle \dots \rangle_{|v_n}$  indicates an average over a large number of events with the same underlying  $v_n$ . The dependence of  $R$  on  $v_n$  can be easily understood if one sees Eq. (2) as a directed random walk: particles are emitted randomly, but the underlying probability distribution (1) is anisotropic. The resolution  $R$  thus depends on the relative magnitude of the anisotropy  $v_n$  to the statistical dispersion  $1/\sqrt{N}$ . In the limit  $v_n \gg 1/\sqrt{N}$  (infinite number of particles), one can exactly reconstruct the underlying event plane so that  $\Phi_n = \Psi_n$ , and

$$R(v_n) \xrightarrow{\text{high res.}} 1. \quad (6)$$

Conversely, when the resolution is low ( $v_n \sqrt{N} \ll 1$ ),

$$R(v_n) \xrightarrow{\text{low res.}} kv_n, \quad (7)$$

where  $k$  is independent of  $v_n$  and scales as  $k \sim \sqrt{N}$ .

In the general case, the value is somewhere in between these limits. Analytic formulas can be obtained for  $R(v_n)$  under rather general assumptions ( $N \gg 1$ ,  $v_n \ll 1$ ,  $v_{2n} \ll 1$ ) [28], but they are of little practical use except when combining subevents.

This nonlinear dependence of the resolution on the underlying flow is the origin of the difficulties of the event-plane method, which arise when flow fluctuations are considered. A simpler quantity is the projection of the flow vector onto the underlying direction  $\Phi_n$ , which directly gives the underlying flow:

$$\left\langle Q_n e^{-in\Phi_n} \right\rangle_{|v_n} = v_n, \quad (8)$$

where we have used Eq. (1).

### B. Correlating subevents

Historically, the most common way to access information about the coefficients  $v_n$  has been so-called event-plane measurements. In these analyses,  $v_n$  is extracted from correlations between particles of interest (e.g., identified particles in a narrow transverse momentum window) and a different set of particles in a reference detector (e.g., unidentified particles in a large  $p_T$  range), typically separated by a gap in pseudorapidity [4, 29].

The event-plane method thus correlates the flow vector of particles of interest, denoted by  $Q_n$ , with the direction

of the flow vector in a reference detector  $A$ , denoted by  $Q_{nA}$ . Assuming that the only correlation between  $Q_n$  and  $Q_{nA}$  is that resulting from their correlation with the direction of anisotropic flow  $\Phi_n$ , this correlation factorizes:

$$\begin{aligned} \left\langle \frac{Q_n Q_{nA}^*}{|Q_{nA}|} \right\rangle_{|v_n} &= \langle Q_n e^{-in\Phi_n} \rangle_{|v_n} \left\langle \frac{Q_{nA}}{|Q_{nA}|} e^{-in\Phi_n} \right\rangle_{|v_n}^* \\ &= v_n R(v_{nA}), \end{aligned} \quad (9)$$

where we have used Eqs. (8) and (5), and  $v_{nA}$  denotes the value of  $v_n$  in the reference detector  $A$ . The resolution  $R(v_{nA})$  is estimated by correlating  $A$  with additional separate reference detectors; Each reference detector is called a ‘‘subevent’’. In the simplest case of two identical subevents ( $A, B$ ) located symmetrically around midrapidity, making use of the factorization hypothesis:

$$\begin{aligned} \left\langle \frac{Q_{nA}}{|Q_{nA}|} \frac{Q_{nB}^*}{|Q_{nB}|} \right\rangle_{|v_n} &= \left\langle \frac{Q_{nA}}{|Q_{nA}|} e^{-in\Phi_n} \right\rangle_{|v_n} \left\langle \frac{Q_{nB}}{|Q_{nB}|} e^{-in\Phi_n} \right\rangle_{|v_n}^* \\ &= \left| \left\langle \frac{Q_{nA}}{|Q_{nA}|} e^{-in\Phi_n} \right\rangle_{|v_n} \right|^2 \\ &= R(v_{nA})^2, \end{aligned}$$

where we have again used Eq. (5). The event-plane measurement is thus defined as

$$v_n\{EP\} \equiv \frac{\left\langle \frac{Q_n Q_{nA}^*}{|Q_{nA}|} \right\rangle}{\sqrt{\left\langle \frac{Q_{nA}}{|Q_{nA}|} \frac{Q_{nB}^*}{|Q_{nB}|} \right\rangle}}, \quad (11)$$

Since it is impossible to select events according to the underlying probability distribution, the measurement is taken with averages over all events in a centrality class, denoted by unadorned angular brackets. In the absence of flow fluctuations (i.e., if the underlying  $v_n$  is the same in every event), Eqs. (9) and (10) ensure that  $v_n\{EP\}$  coincides with the underlying  $v_n$ , up to experimental errors.

A slight variant of the event-plane method consists in removing the factors of  $|Q_n|$  before taking the average in the numerator and denominator of Eq. (11).

$$v_n\{SP\} \equiv \frac{\langle Q_n Q_{nA}^* \rangle}{\sqrt{\langle Q_{nA} Q_{nB}^* \rangle}}, \quad (12)$$

The numerator of Eq. (12) involves a scalar product of two vectors  $\vec{Q}_n \cdot \vec{Q}_{nA}$ , and so is referred to as the scalar-product method [20]. In the absence of flow fluctuations, factorization again applies:

$$\begin{aligned} \langle Q_n Q_{nA}^* \rangle_{|v_n} &= \langle Q_n e^{-in\Phi_n} \rangle_{|v_n} \langle Q_{nA} e^{-in\Phi_n} \rangle_{|v_n}^* \\ &= v_n v_{nA} \end{aligned} \quad (13)$$

and similarly

$$\langle Q_{nA} Q_{nB}^* \rangle_{|v_n} = v_{nA}^2. \quad (14)$$

Therefore  $v_n\{SP\}$  also coincides with the underlying  $v_n$  in the absence of flow fluctuations.

### C. Flow fluctuations

However, it is now known that  $v_n$  fluctuates significantly from event to event [14]. To make it clear what is really measured in this case, we evaluate event averages in two steps, by first averaging over events with the same  $v_n$ , then combining bins of  $v_n$ .

$$\langle \dots \rangle \equiv \left\langle \left\langle \dots \right\rangle_{|v_n} \right\rangle_{v_n}. \quad (15)$$

We apply this decomposition to Eq. (11) and evaluate the inner average using Eqs. (9) and (10):

$$v_n\{EP\} = \frac{\langle v_n R(v_{nA}) \rangle_{v_n}}{\sqrt{\langle R(v_{nA})^2 \rangle_{v_n}}}, \quad (16)$$

Note that  $\langle R(v_{nA})^2 \rangle \neq \langle R(v_{nA}) \rangle^2$ , so that the resolution correction is no longer a simple projection of the measured event plane  $\Psi_n$  onto the ‘‘true’’ event plane  $\Phi_n$ .

In the limit of perfect resolution (i.e., the number of particles used in the reference detector goes to infinity),  $R(v_{nA}) \simeq 1$  and  $v_n\{EP\}$  does indeed measure the event-averaged mean  $v_n$  from Eq. (1),

$$v_n\{EP\} \xrightarrow{\text{high res.}} \langle v_n \rangle. \quad (17)$$

In reality, the resolution is not perfect, and the result is usually closer to the low resolution limit [16]. In this limit,  $R(v_{nA}) \propto v_{nA}$ . Assuming that flow fluctuations are global, i.e.,  $v_n/v_{nA}$  does not fluctuate significantly, the event-plane measurement thus yields a root-mean-square value,

$$v_n\{EP\} \xrightarrow{\text{low res.}} \sqrt{\langle v_n^2 \rangle}. \quad (18)$$

In general, the event-plane method yields a result which may lie anywhere between the two limits (17) and (18). The exact measured quantity depends the detector acceptance—even after the resolution correction is applied—so that the measurement is ambiguous.

The difference between the two limits ranges from 6 to 13%, as illustrated in Fig. 1. As the field enters an era of precision physics, comparisons of different experimental analyses [17] and of theory to experiment [33] are significantly complicated by this dependence on analysis details. For example, the large detector acceptance and high multiplicities of recent measurements at the LHC allow for a larger resolution than was available at RHIC. The natural choice (and what has been done) is to take advantage of this extra resolution to minimize the statistical uncertainty of the measurement. The penalty, however, is that comparisons to earlier measurements become ambiguous, and one has difficulty determining from these measurements how much the flow changes, e.g., with collision energy.

Theoretical comparisons are hampered for the same reason. Theorists have access to more information than

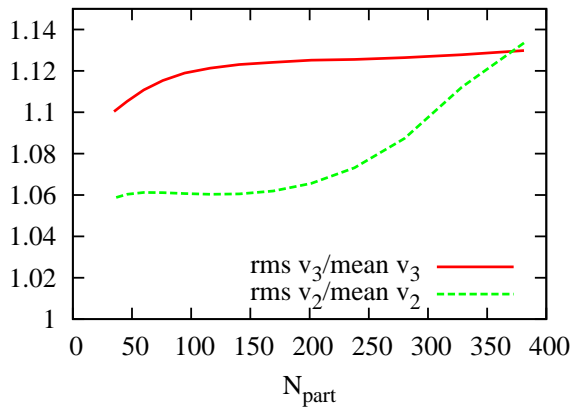


FIG. 1. (Color online) Ratio of the rms  $v_n$ , corresponding to the low-resolution limit of Eq. (11) integrated over  $p_T$ , to the mean  $v_n$ , corresponding to the high-resolution limit, as a function of the number of participant nucleons (binned in 5% centrality intervals), for a Pb-Pb collision at 2.76 TeV per nucleon pair. We model flow fluctuations by assuming  $v_n \propto \varepsilon_n$  in each event, where  $\varepsilon_n$  is the anisotropy of the initial distribution in the corresponding harmonic, defined as in Ref. [30]. The value of  $\varepsilon_n$  in each event is obtained from the Phobos Monte Carlo Glauber model [31]. For  $v_3$ , the ratio is close to  $2/\sqrt{\pi} \simeq 1.13$ , corresponding to Gaussian fluctuations [32].

experiments — their ‘detectors’ have perfect efficiency and suffer no dead spots or holes in coverage; i.e., they can see all particles that are produced. However, if they succumb to the temptation to make use of this extra information to improve statistics (or they simply lack detailed information about detector performance to appropriately degrade the data) comparisons to measurements can become ambiguous and unreliable — even if they otherwise follow the exact same procedures as the experiment [34–36].

Fortunately, this ambiguity can be removed by using the scalar-product method. Although it was originally introduced for unrelated reasons, it gives a well-defined measurement in the presence of flow fluctuations [17], despite differing only trivially from the traditional analysis. When  $v_n$  fluctuates, we again apply the decomposition (15) to Eq. (12) and evaluate the numerator and the denominator using Eqs. (13) and (14):

$$v_n\{SP\} = \frac{\langle v_n v_{nA} \rangle v_n}{\sqrt{\langle v_{nA}^2 \rangle v_n}} = \sqrt{\langle v_n^2 \rangle}, \quad (19)$$

where we have again used the hypothesis that  $v_n/v_{nA}$  does not fluctuate significantly. Therefore, the scalar-product method always yields the root-mean-square  $v_n$ , regardless of the details of the analysis, and makes for a superior measurement.

One can also choose to measure a two-particle correlation [37], which is essentially equivalent to a scalar-product analysis, and also always measures this same un-

ambiguous root-mean-square value [13]. It is important to emphasize, however, that even when an event-plane-type analysis is preferred for practical reasons, only a trivial change to the standard analysis is required in order to obtain a well-defined observable.

If the resolution is large enough, higher-order cumulants [18, 19] can be analyzed. These then yield an unambiguous measurement of higher-order, even moments of the distribution of  $v_n$ , i.e.  $\langle (v_n)^{2k} \rangle$  [13]. Since a standard event-plane method measures a quantity that is different from any of these individual observables, one might naively think it useful to perform both analyses in order to obtain the maximum amount of independent information. However, it has been proven [17] that the event-plane method, in addition to being ambiguous, contains no independent information beyond that contained in the first two cumulants,  $v_n\{2\}$  and  $v_n\{4\}$  (regardless of whether nonflow correlations are present in the system). So there is no reason to use a standard event-plane method in any future analysis.

#### D. Practical details

Actual measurements often differ slightly from the above idealized discussion. The flow vector (3) is typically defined [9] without the normalization factor  $N$ . Similarly, the numerators in Eqs. (11) and (12) are calculated as a sum over the particles of interest in all events, before normalizing by the total number of particles after the sum over events. Thus, there are weighting factors of  $N$  and  $dN/dp_T$ , respectively, inside the event averages, which become important only if large enough centrality bins are used such that multiplicity and spectrum fluctuations are significant.

Second, the flow vector used to estimate the event plane is often calculated as a weighted average of particles. In particular, if it is measured using a calorimeter, the particles are weighted according to their energy, while a  $p_T$ -dependent weight is often used to increase the resolution or to remove non-flow correlations [38]. In this case  $v_{nA}$  above refers to a weighted average.

Third, in the case where identical subevents are not available, the analysis can be done with three arbitrary subevents  $A$ ,  $B$ , and  $C$  [9]. One then does the following replacement

$$\langle Q_{nA} Q_{nB}^* \rangle \rightarrow \frac{\langle Q_{nA} Q_{nB}^* \rangle \langle Q_{nA} Q_{nC}^* \rangle}{\langle Q_{nB} Q_{nC}^* \rangle} \quad (20)$$

in the denominator of Eq. (12), and a similar modification in the resolution correction of Eq. (11).

Fourth, we have used a complex notation throughout this section. However, all quantities are real after averaging over events, except for irrelevant experimental errors. Therefore  $\langle \dots \rangle$  should be replaced by  $\Re \langle \dots \rangle$  everywhere.

Finally, if any of the flow vectors in the numerator of Eqs. (11) and (12) are calculated from the same or over-

lapping sets of particles, care must be made to remove self-correlations [27].

### E. Combining subevents

We end this section with a brief description of how the precision of the scalar-product method can be improved beyond previous implementations. Since at least two reference detectors  $A$  and  $B$  are needed in order to carry out the flow analysis, it is tempting to combine the information from both detectors into a single measurement with reduced statistical uncertainty. In the standard event-plane method, this can be done for identical subevents at the expense of additional hypotheses and algebraic complications [9, 28], but there is no known way of recombining non-identical subevents, as in the three-subevent method.

With the scalar-product method, combining measurements from two reference detectors  $A$  and  $B$  is straightforward, even if they are not identical. One simply measures  $v_n$  independently with respect to  $A$  and to  $B$ . By linearity of the scalar product, combining both measurements (denoted by  $v_n\{SP, A\}$  and  $v_n\{SP, B\}$ ) amounts to taking a weighted average. We show in Appendix A that the optimal weighting is

$$v_n\{SP\} \equiv \frac{\chi_A^2 v_n\{SP, A\} + \chi_B^2 v_n\{SP, B\}}{\chi_A^2 + \chi_B^2}, \quad (21)$$

where  $\chi_A$  is the dimensionless resolution parameter. For identical subevents,  $v_n$  is the mean of  $v_n\{SP, A\}$  and  $v_n\{SP, B\}$  by symmetry:

$$v_n\{SP\} = \frac{v_n\{SP, A\} + v_n\{SP, B\}}{2}. \quad (22)$$

For non-identical subevents, a third subevent  $C$  is required in order to determine the resolution parameter:  $\chi_A$  is given by

$$\frac{1}{\chi_A^2} + 1 \equiv \frac{\langle (\vec{Q}_{nA})^2 \rangle \langle \vec{Q}_{nB} \cdot \vec{Q}_{nC} \rangle}{\langle \vec{Q}_{nA} \cdot \vec{Q}_{nB} \rangle \langle \vec{Q}_{nA} \cdot \vec{Q}_{nC} \rangle}, \quad (23)$$

and  $\chi_B$  is given obtained through the substitution  $A \leftrightarrow B$  in Eq. (23). Note that when detectors are combined, their resolution parameters  $\chi$  add in quadrature. Generalization of Eq. (21) to three subevents  $A$ ,  $B$  and  $C$  is straightforward.

### III. HIGHER-ORDER CORRELATIONS

Fourier harmonics of the azimuthal distribution are now measured up to  $v_4$  [10] at RHIC and up to  $v_5$  [6, 39] and  $v_6$  [7] at LHC. Much additional information is contained in mixed correlations between different harmonics [40–43], which give information about event plane angles  $\Phi_n$  and will likely play a large part in upcoming

measurements. Before rushing into analysis, it is important to define observables for good measurements, which will allow unambiguous comparison between different experiments, and with theory.

The ATLAS collaboration has recently released preliminary measurements of an extensive set of correlations between event planes using traditional methods [23]. For illustration, we consider the first of these correlations. It is a correlation between the event planes  $\Psi_4$  and  $\Psi_2$ , namely,  $\langle \cos 4(\Psi_4 - \Psi_2) \rangle$ , which is then divided by a resolution factor in order to unravel the correlation between the underlying reference directions  $\Phi_4$  and  $\Phi_2$ . They thus write:

$$\langle \cos 4(\Phi_4 - \Phi_2) \rangle = \frac{\langle \cos 4(\Psi_4 - \Psi_2) \rangle}{\langle \cos 4(\Psi_4 - \Phi_4) \rangle \langle \cos 4(\Psi_2 - \Phi_2) \rangle}. \quad (24)$$

This equation is based on the same hypotheses as the event-plane method, which fail if  $v_2$  and  $v_4$  fluctuate. Specifically, the numerator of the right-hand side does not factorize into  $\langle \cos 4(\Psi_4 - \Phi_4) \rangle \langle \cos 4(\Psi_2 - \Phi_2) \rangle$ , and the resolution corrections estimated using standard procedures do not actually correspond to  $\langle \cos 4(\Psi_4 - \Phi_4) \rangle$  and  $\langle \cos 4(\Psi_2 - \Phi_2) \rangle$ .

Using the notations introduced in the previous section, and assuming symmetric subevents  $A$  and  $B$  for simplicity, the observable actually measured is

$$\langle \cos 4(\Phi_4 - \Phi_2) \rangle \{EP\} \equiv \frac{\left\langle \frac{Q_{4A} Q_{2B}^*}{|Q_{4A}| |Q_{2B}|} \right\rangle}{\sqrt{\left\langle \frac{Q_{4A} Q_{4B}^*}{|Q_{4A}| |Q_{4B}|} \right\rangle} \sqrt{\left\langle \frac{Q_{2B}^2 Q_{2A}^*}{|Q_{2B}| |Q_{2A}|} \right\rangle}}. \quad (25)$$

In the presence of flow fluctuations, the average over events can be evaluated in two steps following (15). In addition to  $R_n$  given by Eq. (5), we define a similar quantity  $\mathcal{R}_n$

$$\mathcal{R}_n \equiv \sqrt{\langle e^{2in(\Psi_n - \Phi_n)} \rangle_{|v_n}} = \sqrt{\left\langle \left( \frac{Q_n}{|Q_n|} e^{-in\Phi_n} \right)^2 \right\rangle_{|v_n}} \quad (26)$$

which has the same limits, Eqs. (6) and (7), but can differ at an arbitrary resolution. With this notation,

$$\langle \cos 4(\Phi_4 - \Phi_2) \rangle \{EP\} = \frac{\langle R_4 \mathcal{R}_2^2 e^{4i(\Phi_4 - \Phi_2)} \rangle_{v_n}}{\sqrt{\langle R_4^2 \rangle_{v_n}} \sqrt{\langle \mathcal{R}_2^4 \rangle_{v_n}}} \quad (27)$$

In the limit where the resolutions on both harmonics are perfect, the quantity measured by ATLAS is indeed the nominal value, corresponding to the left-hand side of Eq. (24):

$$\cos 4(\Psi_4 - \Psi_2) \{EP\} \xrightarrow{\text{high res.}} \langle \cos 4(\Phi_4 - \Phi_2) \rangle. \quad (28)$$

In the limit of low resolution, however, repeating the same reasoning as in the previous section, what is ac-

tually measured is the quantity

$$\cos 4(\Psi_4 - \Psi_2)\{EP\} \xrightarrow{\text{low res.}} \frac{\langle v_{4A} v_{2A}^2 \cos 4(\Phi_4 - \Phi_2) \rangle}{\sqrt{\langle v_{4A}^2 \rangle \langle v_{2A}^4 \rangle}}. \quad (29)$$

As before, the measured value is generally between the two limits.<sup>1</sup> Similar expressions can be written for the other correlations in the large set measured by ATLAS. Unlike measurements of  $v_n\{EP\}$ , however, there is no known way to even estimate where between these limits the result lies based only on the reported event-plane resolution.

Note that the same ambiguity plagues previous measurements of the similar ( $p_T$ -differential) quantity,  $v_4$  with respect to the event-plane of elliptic flow  $\Psi_2$  [21, 22]. Not only does the result depend on the resolution, it also depends on how the resolution correction is defined, as the seminal paper [9] proposes two possible implementations, which turn out to be different in the presence of flow fluctuations.

The high resolution limit of these measurements is the nominal quantity

$$v_4\{\Psi_2\} \xrightarrow{\text{high res.}} \langle v_4 \cos 4(\Phi_4 - \Phi_2) \rangle. \quad (30)$$

The low-resolution limit depends on the actual implementation of the resolution correction. STAR [21] uses Eq. (11) of [9], which reduces to

$$v_4\{\Psi_2\} \xrightarrow{\text{low res.}} \frac{\langle v_4 v_{2A}^2 \cos 4(\Phi_4 - \Phi_2) \rangle}{\langle v_{2A}^2 \rangle} \quad (31)$$

in the low-resolution limit, where again  $v_{2A}$  is integrated over the reference detector. PHENIX uses the same implementation as ATLAS (Eq. (14) or Eq. (16) of [9]) which yields, in the low-resolution limit,

$$v_4\{\Psi_2\} \xrightarrow{\text{low res.}} \frac{\langle v_4 v_{2A}^2 \cos 4(\Phi_4 - \Phi_2) \rangle}{\sqrt{\langle v_{2A}^4 \rangle}}. \quad (32)$$

As recently demonstrated in Ref. [33] in full event-by-event hydrodynamic calculations, this ambiguity of the event-plane method is a significant source of uncertainty when comparing experiment to theory. In fact, it should already have been apparent that the effect of detector resolution in measurements such as these is much larger than for the  $v_n\{EP\}$  measurements described above. The difference between Eqs. (31) and (32) likely explains why the values of  $v_4\{\Psi_2\}$  are systematically higher for STAR than for PHENIX by some 10% [24]. In Ref. [21] the STAR collaboration measured  $v_4\{\Psi_2\}$ , but in addition measured a 3-particle correlation  $v_4\{3\}$ , which corresponds to the low-resolution limit of their event-plane

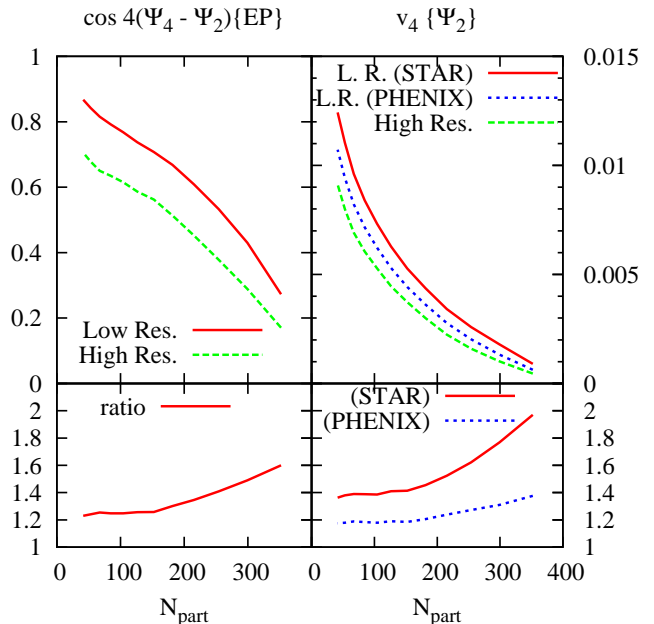


FIG. 2. (Color online) Top, left: low and high resolution limits of the correlation between  $\Phi_2$  and  $\Phi_4$ , defined by Eqs. (29) and (28), versus number of participants. Top, right: low and high resolution limits for integrated  $v_4\{\Psi_2\}$ , defined by Eqs. (31), (32) and (30). Bottom panels: ratios of the low-resolution to high-resolution results. The nominally-measured values correspond to the high-resolution limit, which can differ from what is actually measured (usually closer to the low-resolution limit) by up to a factor 2.

measurement. The STAR collaboration finds that  $v_4\{3\}$  is larger than  $v_4\{\Psi_2\}$  by 20% for mid central collisions. This difference is much larger than the difference between, e.g.,  $v_2\{EP\}$  and the low resolution limit  $v_2\{SP\}$  in the same experiment (which is roughly 5%).

In order to illustrate the possible full dependence on resolution, we use here a simplified calculation, though the results are consistent with more sophisticated calculations [33]. It is known from event-by-event hydrodynamic calculations that  $p_T$ -integrated  $v_2$ ,  $v_4$ , and the corresponding reference directions  $\Phi_2$  and  $\Phi_4$  can be accurately predicted in each event from the initial eccentricities according to [30]

$$\begin{aligned} v_2 e^{2i\Phi_2} &= a \varepsilon_2 e^{2i\Phi_{in,2}} \\ v_4 e^{4i\Phi_4} &= b \varepsilon_4 e^{4i\Phi_{in,4}} + c (\varepsilon_2 e^{2i\Phi_{in,2}})^2, \end{aligned} \quad (33)$$

where  $a$ ,  $b$ ,  $c$  are real coefficients, and  $\varepsilon_n$  and  $\Phi_{in,n}$  are the initial anisotropy in harmonic  $n$  and its reference direction, as defined in Ref. [30].

We thus compute  $\varepsilon_n$  and  $\Phi_{in,n}$  using the PHOBOS Monte Carlo Glauber [31] and take the values of  $b$  and  $c$  from the viscous hydrodynamic calculation by Teaney and Yan [43], for simplicity taking centrality-independent

<sup>1</sup> Note that the low-resolution limit (29) lies between  $-1$  and  $+1$  by construction, even though it does not reduce to a simple angular correlation.

values of  $b = 0.018$  and  $c = 0.07$ <sup>2</sup>.

The right-hand side of Eqs. (28) and (29) are displayed in Fig. 2 (top, left), as well with their ratio (bottom, left), and similarly for Eqs. (30), (31) and (32) on the right side of the figure. The ratio varies from 1.4 to more than 2 (in agreement with full event-by-event hydrodynamic calculations of  $v_4\{\Psi_2\}$  [33]). Comparing with Fig. 1, one sees that the ambiguity induced by the event-plane method is much worse for mixed correlations than for individual measurements of  $v_n$ .

As a recent illustration of the problems that can arise from this, we point to the correlations calculated in Ref. [44], corresponding to the high resolution limit of the recent preliminary ATLAS measurements — i.e., the quantities that were nominally claimed as measured. They are all clearly smaller in magnitude than the measurements, despite each observable having the correct sign and centrality dependence. Naively, this seems to indicate that the theory needs to be changed somehow to accommodate this difference, but in fact the finite resolution of the experiment could in principle explain the entire discrepancy. Further, while it is straightforward to calculate either the low or the high resolution limit, as done in that work, a calculation that reliably corresponds exactly to the measured quantity adds considerable difficulty. In fact, it is not possible without access to more information about the experimental details than is available.

Fortunately, the ambiguity of the event-plane method can easily be removed by using a straightforward generalization of the scalar-product method. The right-hand side of Eq. (29) is given by

$$\frac{\langle v_{4A} v_{2A}^2 \cos 4(\Phi_4 - \Phi_2) \rangle}{\langle v_{2A}^2 \rangle \sqrt{\langle v_{4A}^2 \rangle}} = \frac{\langle Q_{4A} Q_{2B}^{*2} \rangle}{\sqrt{\langle Q_{4A} Q_{4B}^* \rangle} \sqrt{\langle Q_{2B}^2 Q_{2A}^{*2} \rangle}}, \quad (34)$$

which we suggest as a replacement for Eq. (25). In the same way as for individual measurements of  $v_n$ , this method yields a result which is unambiguous and independent of the number of particles selected for analysis. Note that the numerator is a sum over all triplets of particles of  $\langle \cos(2\phi_1 + 2\phi_2 - 4\phi_3) \rangle$ . The quantity in Eq. (34) is thus identical to the type of scaled correlations introduced in [40].

Generalization of the above discussion to  $v_4\{\Psi_2\}$  and other mixed correlations [23, 40] is straightforward. In general, higher-order correlations involve higher moments of the distribution of anisotropic flow, and have therefore an increased sensitivity to flow fluctuations.

<sup>2</sup> Note that Teaney and Yan use cumulants of the initial distribution, which are linear combinations of our moments: with their notation,  $b = w_4/C_4$  and  $c = w_{4(22)}/\varepsilon_2^2 + 3(w_4/C_4)\langle r^2 \rangle^2/\langle r^4 \rangle$ . We take  $w_4/C_4 \simeq 0.018$  and  $w_{4(22)}/\varepsilon_2^2 \simeq 0.04$  from their Fig. 2, right, and we estimate  $\langle r^2 \rangle^2/\langle r^4 \rangle \simeq 0.6$  from a Glauber calculation.

Note that the particular correlation between  $\Phi_2$  and  $\Phi_4$  studied above can be contaminated by nonflow correlations; Therefore it is important that the flow vectors  $Q_2$  and  $Q_4$  are determined in regions separated by a pseudorapidity gap [23]. Other mixed correlations, such as the correlation between  $\Phi_2$  and  $\Phi_3$ , are not sensitive to nonflow correlations. The need for gaps in pseudorapidity must be considered on a case-by-case basis [45].

#### IV. CONCLUSION

We have explained that measurements of anisotropic flow using the event-plane method are ambiguous because the result depends on analysis details. This dependence, which is due to event-by-event flow fluctuations, is typically up to a few percent for  $v_2$  and 10% for  $v_3$  and higher harmonics. For mixed correlations involving event planes from different harmonics, the dependence is much larger — we have demonstrated that the result may vary by a factor 2 depending on analysis details. We have shown that these ambiguities of the event-plane method can be repaired with only minor modifications and without any additional complication or drawbacks. We therefore conclude that the traditional event-plane method should be abandoned in future analyses.

#### ACKNOWLEDGMENTS

ML is supported by the European Research Council under the Advanced Investigator Grant ERC-AD-267258. We thank Instituto de Fisica, Sao Paulo, where this paper was written, for hospitality, and FAPESP-CNRS for financial support (project 2011/51864-0)

#### Appendix A: Combining reference flows

In this Appendix, we show that Eq. (21) defines the optimal combination between anisotropic flows measured in detectors  $A$  and  $B$  using the scalar-product method, in the sense that it minimizes the statistical error.

Eq. (12) can be rewritten as

$$v_n\{SP\} = \frac{\langle Q_n Q_{nA}^* \rangle}{\bar{Q}_A}, \quad (A1)$$

(for simplicity, we drop the index  $n$  from now on) where  $\bar{Q}_A$  is the resolution correction in subevent  $A$ , which is generally obtained using three subevents  $A, B, C$  pairwise separated by rapidity gaps:

$$\bar{Q}_A \equiv \sqrt{\frac{\langle Q_A Q_B^* \rangle \langle Q_A Q_C^* \rangle}{\langle Q_B Q_C^* \rangle}}. \quad (A2)$$

Assuming that  $v_n \ll 1$  and that one measures  $v_n$  in a narrow bin which contains at most one particle per event, so

that  $Q$  is essentially a random number on the unit circle, and keeping in mind that one only keeps the real part in the numerator of Eq. (A1), a straightforward calculation shows that the statistical error on  $v_n\{SP\}$  is

$$\delta v = \frac{1}{\sqrt{2N}} \frac{\sqrt{\langle |Q_A|^2 \rangle}}{\bar{Q}_A}, \quad (\text{A3})$$

where  $N$  is the number of particles in the bin.

If one measures  $v_n$  in a detector that is separated in pseudorapidity from both  $A$  and  $B$ , the measurement can be done using either  $A$  or  $B$  as a reference. We denote by  $v\{SP, A\}$  and  $v\{SP, B\}$  the corresponding estimates, where  $v\{SP, A\}$  is given by Eq. (A1) and  $v\{SP, B\}$  is given by substituting  $A \leftrightarrow B$  in Eqs. (A1) and (A2). Note that by definition of  $\bar{Q}_A$  and  $\bar{Q}_B$ ,

$$\langle Q_A Q_B^* \rangle = \bar{Q}_A \bar{Q}_B. \quad (\text{A4})$$

One can combine linearly the flow vectors and the resolution corrections

$$\begin{aligned} Q_{\text{combined}} &\equiv Q_A + \lambda Q_B \\ \bar{Q}_{\text{combined}} &\equiv \bar{Q}_A + \lambda \bar{Q}_B, \end{aligned} \quad (\text{A5})$$

where  $\lambda$  is arbitrary. The resulting combined measurement is

$$v\{SP\} \equiv \frac{\langle Q Q_{\text{combined}}^* \rangle}{\bar{Q}_{\text{combined}}} = \frac{\bar{Q}_A v\{SP, A\} + \lambda \bar{Q}_B v\{SP, B\}}{\bar{Q}_A + \lambda \bar{Q}_B}. \quad (\text{A6})$$

Using Eq. (A3), with  $Q_A$  replaced by  $Q_{\text{combined}}$ , straightforward algebra shows that the value of  $\lambda$  which minimizes the statistical error on  $v\{SP\}$  is

$$\lambda = \frac{\bar{Q}_B \langle |Q_A|^2 \rangle - \bar{Q}_A \langle Q_A Q_B^* \rangle}{\bar{Q}_A \langle |Q_B|^2 \rangle - \bar{Q}_B \langle Q_A Q_B^* \rangle}. \quad (\text{A7})$$

Using Eq. (A4), this can be rewritten

$$\lambda = \frac{\bar{Q}_B (\langle |Q_A|^2 \rangle - \bar{Q}_A^2)}{\bar{Q}_A (\langle |Q_B|^2 \rangle - \bar{Q}_B^2)}. \quad (\text{A8})$$

We now express  $\lambda$  in terms of the resolution parameter, Eq. (23). Using the factorization property Eq. (A4), we rewrite Eq. (23) as

$$\frac{1}{\chi_A^2} + 1 \equiv \frac{\langle |Q_A|^2 \rangle}{\bar{Q}_A^2} \quad (\text{A9})$$

or, equivalently,

$$\chi_A^2 \equiv \frac{\bar{Q}_A^2}{\langle |Q_A|^2 \rangle - \bar{Q}_A^2}. \quad (\text{A10})$$

In the absence of flow fluctuations, the resolution parameter  $\chi_A$  is the ratio of the underlying flow (8) to the standard deviation of the flow vector around the mean flow [28]. Using Eq. (A10), Eq. (A8) can be rewritten as

$$\lambda = \frac{\bar{Q}_A \chi_B^2}{\bar{Q}_B \chi_A^2}, \quad (\text{A11})$$

Inserting this value of  $\lambda$  into Eq. (A6), one recovers Eq. (21).

- 
- [1] K. H. Ackermann *et al.* [STAR Collaboration], Phys. Rev. Lett. **86**, 402-407 (2001) [nucl-ex/0009011].
- [2] B. B. Back *et al.* [PHOBOS Collaboration], Phys. Rev. Lett. **89**, 222301 (2002) [nucl-ex/0205021].
- [3] C. Alt *et al.* [NA49 Collaboration], Phys. Rev. C **68**, 034903 (2003) [nucl-ex/0303001].
- [4] S. S. Adler *et al.* [PHENIX Collaboration], Phys. Rev. Lett. **91**, 182301 (2003) [nucl-ex/0305013].
- [5] K. Aamodt *et al.* [ALICE Collaboration], Phys. Rev. Lett. **105**, 252302 (2010) [arXiv:1011.3914 [nucl-ex]].
- [6] S. Chatrchyan *et al.* [CMS Collaboration], Eur. Phys. J. C **72**, 2012 (2012) [arXiv:1201.3158 [nucl-ex]].
- [7] G. Aad *et al.* [ATLAS Collaboration], Phys. Rev. C **86**, 014907 (2012) [arXiv:1203.3087 [hep-ex]].
- [8] D. Adamova *et al.* [CERES Collaboration], Nucl. Phys. A **894**, 41 (2012) [arXiv:1205.3692 [nucl-ex]].
- [9] A. M. Poskanzer and S. A. Voloshin, Phys. Rev. C **58**, 1671 (1998) [arXiv:nucl-ex/9805001].
- [10] A. Adare *et al.* [PHENIX Collaboration], Phys. Rev. Lett. **107**, 252301 (2011) [arXiv:1105.3928 [nucl-ex]].
- [11] S. Chatrchyan *et al.* [CMS Collaboration], Phys. Rev. C **87**, 014902 (2013) [arXiv:1204.1409 [nucl-ex]].
- [12] B. Abelev *et al.* [ALICE Collaboration], Phys. Lett. B **719**, 18 (2013) [arXiv:1205.5761 [nucl-ex]].
- [13] M. Miller and R. Snellings, nucl-ex/0312008.
- [14] B. Alver *et al.* [PHOBOS Collaboration], Phys. Rev. Lett. **98**, 242302 (2007) [nucl-ex/0610037].
- [15] B. Alver and G. Roland, Phys. Rev. C **81**, 054905 (2010) [Erratum-ibid. C **82**, 039903 (2010)] [arXiv:1003.0194 [nucl-th]].
- [16] B. Alver *et al.*, Phys. Rev. C **77**, 014906 (2008) [arXiv:0711.3724 [nucl-ex]].
- [17] J. -Y. Ollitrault, A. M. Poskanzer, S. A. Voloshin, Phys. Rev. C **80**, 014904 (2009) [arXiv:0904.2315 [nucl-ex]].
- [18] N. Borghini, P. M. Dinh, J. -Y. Ollitrault, Phys. Rev. C **64**, 054901 (2001). [nucl-th/0105040].
- [19] A. Bilandzic, R. Snellings, S. Voloshin, Phys. Rev. C **83**, 044913 (2011). [arXiv:1010.0233 [nucl-ex]].
- [20] C. Adler *et al.* [STAR Collaboration], Phys. Rev. C **66**, 034904 (2002) [nucl-ex/0206001].
- [21] J. Adams *et al.* [STAR Collaboration], Phys. Rev. Lett. **92**, 062301 (2004) [nucl-ex/0310029].
- [22] A. Adare *et al.* [PHENIX Collaboration], Phys. Rev. Lett. **105**, 062301 (2010) [arXiv:1003.5586 [nucl-ex]].
- [23] J. Jia [ATLAS Collaboration], arXiv:1208.1427 [nucl-ex].
- [24] C. Gombeaud and J. -Y. Ollitrault, Phys. Rev. C **81**,



- 014901 (2010) [arXiv:0907.4664 [nucl-th]].
- [25] M. Luzum, J. Phys. G **38**, 124026 (2011) [arXiv:1107.0592 [nucl-th]].
- [26] S. Wang, Y. Z. Jiang, Y. M. Liu, D. Keane, D. Beavis, S. Y. Chu, S. Y. Fung and M. Vient *et al.*, Phys. Rev. C **44**, 1091 (1991).
- [27] P. Danielewicz and G. Odnyc, Phys. Lett. B **157**, 146 (1985).
- [28] J. -Y. Ollitrault, nucl-ex/9711003.
- [29] B. Alver *et al.* [PHOBOS Collaboration], Phys. Rev. C **81**, 034915 (2010) [arXiv:1002.0534 [nucl-ex]].
- [30] F. G. Gardim, F. Grassi, M. Luzum and J. -Y. Ollitrault, Phys. Rev. C **85**, 024908 (2012) [arXiv:1111.6538 [nucl-th]].
- [31] B. Alver, M. Baker, C. Loizides and P. Steinberg, arXiv:0805.4411 [nucl-ex].
- [32] S. A. Voloshin, A. M. Poskanzer, A. Tang and G. Wang, Phys. Lett. B **659**, 537 (2008) [arXiv:0708.0800 [nucl-th]].
- [33] F. G. Gardim, F. Grassi, M. Luzum and J. -Y. Ollitrault, Phys. Rev. Lett. **109**, 202302 (2012) [arXiv:1203.2882 [nucl-th]].
- [34] H. Holopainen, H. Niemi and K. J. Eskola, Phys. Rev. C **83**, 034901 (2011). [arXiv:1007.0368 [hep-ph]].
- [35] H. Petersen, Phys. Rev. C **84**, 034912 (2011). [arXiv:1105.1766 [nucl-th]].
- [36] L. Pang, Q. Wang and X. -N. Wang, Phys. Rev. C **86**, 024911 (2012). [arXiv:1205.5019 [nucl-th]].
- [37] K. Aamodt *et al.* [ALICE Collaboration], Phys. Lett. B **708**, 249 (2012) [arXiv:1109.2501 [nucl-ex]].
- [38] M. Luzum and J. -Y. Ollitrault, Phys. Rev. Lett. **106**, 102301 (2011) [arXiv:1011.6361 [nucl-ex]].
- [39] K. Aamodt *et al.* [ALICE Collaboration], Phys. Rev. Lett. **107**, 032301 (2011) [arXiv:1105.3865 [nucl-ex]].
- [40] R. S. Bhalerao, M. Luzum and J. -Y. Ollitrault, Phys. Rev. C **84**, 034910 (2011) [arXiv:1104.4740 [nucl-th]].
- [41] D. Teaney and L. Yan, Phys. Rev. C **83**, 064904 (2011) [arXiv:1010.1876 [nucl-th]].
- [42] R. S. Bhalerao, M. Luzum and J. -Y. Ollitrault, Phys. Rev. C **84**, 054901 (2011) [arXiv:1107.5485 [nucl-th]].
- [43] D. Teaney and L. Yan, Phys. Rev. C **86**, 044908 (2012) [arXiv:1206.1905 [nucl-th]].
- [44] Z. Qiu and U. Heinz, Phys. Lett. B **717**, 261 (2012) [arXiv:1208.1200 [nucl-th]].
- [45] R. S. Bhalerao, M. Luzum and J. Y. Ollitrault, J. Phys. G **38**, 124055 (2011) [arXiv:1106.4940 [nucl-ex]].